Polímeros
ISSN 1678-5169 (Online)

https://doi.org/10.1590/0104-1428.20250001

ORIGINAL ARTICLES

Green synthesis of N-doped carbon dots from cocoa fruit skin as antibacterial

Marpongahtun[1]*, Amru Daulay[2], Putri[3], Aniza Salviana Prayugo[4], Roon Goei[5], Salmiati[6]

[1]Department of Chemistry, Faculty of Mathematics and Natural Sciences, Universitas Sumatera Utara, Medan, Indonesia

[2]Research Center for Mining Technology, National Research and Innovation Agency – BRIN, Lampung Province, Indonesia

[3]Department of Chemistry, Faculty of Mathematics and Natural Sciences, Graduate School, Universitas Sumatera Utara, Medan, Indonesia

[4]Department of Chemistry, Faculty of Mathematics and Natural Sciences, Postgraduate School, Universitas Sumatera Utara, Medan, Indonesia

[5]School of Material Science and Engineering, Nanyang Technological University, Singapore, Singapore

[6]Department of Environmental Engineering, Universitas Sumatera Utara, Medan, Indonesia

**marpongahtun@usu.ac.id*

Abstract

Organic pollutants can be broken down by photocatalysis with the help of carbon dots. Also, it is widely used as a material to stop microorganisms from growing. This study synthesized N-doped carbon dots from cocoa fruit skin as a potential antibacterial. TEM images on N-CDs show the material is dispersed well without forming aggregation. The spacing of the lattice fringe formed is around 0.23 nm, corresponding to graphite's diffraction. FTIR spectra show adsorption peak difference between CDs and N-CDs is 1118 cm^{-1}, indicating C-N stretching. UV-Vis absorption spectrum shows the formation of a peak at 294 nm, which shows the π-π* transition of sp^2, PL QY of N–CDs in a water solution was about 18.25%. It has been seen that N-CDs work very quickly and kill many bacteria compared to CDs. In both CDs, the highest value for the zone of inhibition is 100 μg mL^{-1}.

Keywords: *antibacterial, cocoa fruit skin, nitrogen-doped carbon dots, Theobroma cacao L.*

Data Availability: All data supporting the findings of this study are available from the corresponding author upon request.

How to cite: Marpongahtun, Daulay, A., Putri, Prayugo, A. S., Goei, R., & Salmiati. (2025). Green synthesis of N-doped carbon dots from cocoa fruit skin as antibacterial. *Polímeros: Ciência e Tecnologia*, *35*(4), e20250040. https://doi.org/10.1590/0104-1428.20250001

1. Introduction

Biomass, a renewable resource, demonstrates advantages in biotechnology processes, corrosion inhibition, and pharmaceutical formulation development. Cocoa fruit skin comes from a plant called *Theobroma cacao* L., which is a biomass derived from plants in the Malvaceae family. It contains bioactive compounds such as polyphenols, flavonoids, and tannins that may not be present in some types of lignocellulosic biomass[1]. The utilization of cocoa husks is increasingly expanding, including as animal feed[2] and activated carbon nanoparticles for energy storage devices[3].

Zero-dimensional carbon nanoparticles (<10 nm) known as carbon dots (CDs) consist of a core and shell structure[4]. This material is used as an alternative to fluorescent semiconductor quantum dots, metal NPs/metal oxides, and other nanoparticles, due to its biocompatibility, hydrophilicity, low toxicity, and tunable surface functional groups. CDs have been implemented as sensitizers in solar cells, sensors for detection of heavy metals, organics, and bacteria, and in many other applications[5]. CDs can be made in many ways, such as by acid oxidation[6], laser ablation[7], hydrothermal[8], microwave treatment[9], electrochemical[10], and solvothermal[11]. CDs have been made using green carbon from fruit biomass, vegetables, milk, sugar, and honey[12]. Natural carbon sources like plants, roots, leaves, fruits, and waste products are also used to make N-doped carbon dots (N-CDs)[13]. In particular, the N-CDs have improved the quantum yield, and both the amine and carboxyl groups help make the CDs highly stable. Also, CDs are widely used for their healing properties[14]. Microorganisms can be stopped from growing when they are made of carbon. CDs could be used to stop diseases caused by germs and fungi. Also, these studies on bacteria can help make antibacterial antibiotics and ingredients.

Regarding CDs using biomass and by-products, Thariq's team[15] prepared CDs using figs (Ficus religiosa tree) as raw material through chloroform as solvent. Chloroform

interaction with CDs can alter their properties and ultimately affect their quantum yield[16]. Meng et al.[17] obtained a good water solubility of N-CDs through coke powder and H_2SO_4 and HNO_3 as raw materials and solvents. Using strong oxidizing acids is hazardous for the environment and impurifies the sample mixture[13]. Saravanan et al.[18] created CDs using turmeric leaves as raw material and their potential antibacterial activities. CDs synthesized from natural precursors often exhibit low fluorescence quantum yields. Nitrogen doping can enhance the optical properties of CDs, including increasing fluorescence[19].

It would be good to make biogenic CDs from natural plants and waste materials and study antibacterial properties. This study considered these goals when it chose cocoa fruit skin as the carbon source to make N-CDs. Also, the cocoa fruit skin has many alkaloids, flavonoids, tannins, saponins, and polyphenols. The solvothermal method was used to synthesise CDs from the cocoa fruit skin. This study has also made N-CDs with urea and cocoa fruit skin using the solvothermal method. This study also used N-CDs as antibiotic agents to stop the growth of *Staphylococcus aureus* and *Escherichia coli*. Conclude that N-CDs were good at stopping the growth of germs by acting as antibacterial agents.

2. Materials and Methods

2.1 Materials

Cocoa fruit skin was obtained from Batubara Regency, Indonesia. Urea ($CO(NH_2)_2$ 98wt%), ethanol (C_2H_6O 99wt%), hydrochloric acid (HCl 37wt%), ferric chloride ($FeCl_3$ 97wt%), sodium hydroxide (NaOH 98wt%), ammonia (NH_3 25wt%), chloroform ($CHCl_3$ 99wt%), magnesium (Mg 99wt%), sulfuric acid (H_2SO_4 99 wt%), phosphate-buffered saline (PBS pH 7.4), Mayer's reagent, and Dragendorf reagent were purchased by Sigma-Aldrich. Deionized water (18.2 MΩ/cm) was purchased from CV. Rudang Jaya. Bacteriological agar and yeast extract were obtained from Universitas Sumatera Utara. At the same time, tryptone and sodium chloride were used to prepare Luria broth and agar media for culturing *Escherichia coli* (gram-negative ATCC 25922) and *Staphylococcus aureus* (gram-positive ATCC 23235) bacteria were purchased from Sigma-Aldrich. All chemicals were of analytical grade and were used as received without further purification.

2.2 Preparation of cocoa fruit skin

Cocoa pods that have been obtained are washed with deionized water. Then it was dried using an oven at a temperature of 65 °C. The dried cocoa pods were smoothed using a blender until smooth into powder. After getting the cocoa pod skin powder, it was sifted using a 40-mesh sieve. Then the maceration process was carried out with a sample ratio of 1: 10 in 70% ethanol for 72 h with several stirrings and filtered using filter paper.

2.3 Synthesis of carbon dots

A cocoa fruit skin was put into a 25 mL autoclave with a Teflon-lined autoclave and heated at 220 °C for 2 h. After cooling to room temperature, the solution was centrifuged for 20 min at 8000 rpm. The solution was dialyzed for 48 h by changing the water every 4 h. This sample was named CDs.

2.4 Synthesis of N-doped carbon dots

A cocoa fruit skin of 50 mL added with 2 m/v% urea, was mixed while stirring for 10 min at 240 rpm. The resultant solution was put into a 25 mL autoclave with a Teflon-lined autoclave and heated at 220 °C for 2 h. After cooling to room temperature, the solution was centrifuged for 20 min at 8000 rpm. The solution was dialyzed for 48 h by changing the water every 4 h . The filtrate was stored in a dark container. This sample was named N-CDs.

2.5 Phytochemical analysis of cocoa fruit skin

Alkaloid test using procedure: put enough cocoa fruit skin into the Erlenmeyer, then add 10 mL of ammonia and 10 mL of chloroform. Stir for a few minutes. Then 10 mL of 2N HCl was added and shaken, then divided into 3 test tubes, (i) tube 1 was dripped with Bouchardart reagent, (ii) tube 2 was dripped with Mayer's reagent, and (iii) tube 3 was dripped with Dragendorf reagent. Flavonoid test using procedure: (i) tube 1 was put into a test tube added with 5% $FeCl_3$ and 10% NaOH, (ii) tube 2 was adding of concentrated HCl and Mg powder to the cocoa fruit skin, and (iii) tube 3 adding H_2SO_4 to the cocoa fruit skin. Saponin test using procedure: the cocoa fruit skin was put into a test tube, added deionized water was, and then shaken for 3 min. Tannin Test using procedure: cocoa fruit skin was put into a test tube and added with 5% of $FeCl_3$. Polyphenol test using procedure: cocoa fruit skin was put into a test tube and added with 5% of $FeCl_3$. The terpenoid test using the procedure: (i) tube 1 was cocoa fruit skin added Liebermann-Burchard reagent, and (ii) tube 1 was cocoa fruit skin added Salkowsky reagent.

2.6 Characterization of CDs and N-CDs

High resolution transmission electron microscopy (HRTEM) images were collected using a JEOL-2100 TEM (operated at an accelerating voltage of 200 kV). The fourier-transform infrared spectroscopy (FTIR) spectra were recorded using a PerkinElmer spectrometer in the spectral range of 4000 cm^{-1} - 700 cm^{-1} at the ambient temperature. The optical absorption spectra were recorded using a Shimadzu UV-1800 spectrophotometer. Photoluminescence (PL) spectra of the samples were collected using a single-beam PerkinElmer LS45 fluorescence spectrometer. X-ray Diffraction (XRD) analysis was performed on solid-state Carbon Dots (CDs) samples using a Rigaku MiniFlex II instrument. Energy-dipersive X-ray (EDX) spectra were recorded using EDAX TSL system operated at 20 kV accelerating Volatage. Antibacterial studies of Gram-negative and Gram-positive were examined in the biological laboratory at Universitas Sumatera Utara.

3. Results and Discussions

3.1 Preparation of N-CDs

Phytochemical analysis was carried out on cocoa fruit skin to ensure whether the cocoa fruit skin content was genuinely pure. Cocoa fruit skin contains alkaloids, flavonoids, tannins, saponins, polyphenols, and others. The results of the phytochemical analysis of cocoa fruit skin can be seen in Figure 1. At alkaloid test (Figure 1a) show

a brown precipitate then it is for tube 1, a yellowish-white precipitate for tube 2, and a brick-red precipitate for tube 3. All the tube tests show positive for alkaloids. The flavonoid test (Figure 1b) shows a green solution for tube 1, an orange solution for tube 2, and a red brick solution for tube 3. All the tube tests show positive for flavonoid. The saponin test (Figure 1c) shows that the foam is formed. It concludes the positive for saponin. The tannin test (Figure 1d) shows that a green solution is formed. It shows that a positive for tannin. The polyphenol test (Figure 1e) shows that a black solution is formed. It shows that a positive for polyphenol. The terpenoid test (Figure 1f), in tube 1, shows a two-phase solution with a yellow color at the bottom and brownish yellow at the top which shows negative for terpenoids. Use the Liebermann-Burchard reagent in the terpenoid test to determine the presence of cholesterol in cocoa fruit skin[20]. The results did not show the presence of cholesterol. Tube 2 shows a red solution which indicates positive terpenoids. The results of screening phytochemical cocoa fruit skin can be seen in Table 1.

In synthesizing CDs and N-CDs, a solvothermal reaction at 220°C is used for carbonization to produce fluorescent CDs. The scheme illustration synthesis N-CDs with the solvothermal method can be seen in Figure 2. The fundamental difference between hydrothermal and solvothermal is the solution used. Hydrothermal prefers to use H_2O solutions, while solvothermal uses solutions other than H_2O[21]. The similarities between hydrothermal and solvothermal are using an autoclave to carry out the reaction[22]. The synthesis process yielded 25 mL of purified CDs solution from 2.0 g of cocoa fruit skin powder as the raw material.

Table 1. Screening phytochemical of cocoa fruit skin.

	Method	Result
Alkaloid	Maeyer	+
	Bouchardart	+
	Dragendorff	+
Flavonoid	H_2SO_4	+
	Mg.HCl	+
	$FeCl_3$	+
Terpenoid	Liebermann-Burchard	-
	Salkowsky	+
Saponin	Aquadest	+
Tanin	$FeCl_3$	+
Polifenol	$FeCl_3$	+

+: Positive; -: Negative.

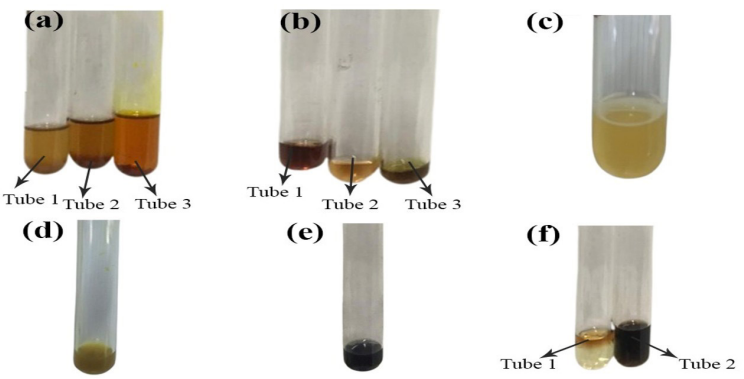

Figure 1. Phytochemical analysis on cocoa fruit skin of (a) alkaloid test, (b) flavonoid test, (c) saponin test, (d) tannin test, (e) polyphenol test, and (f) terpenoid test.

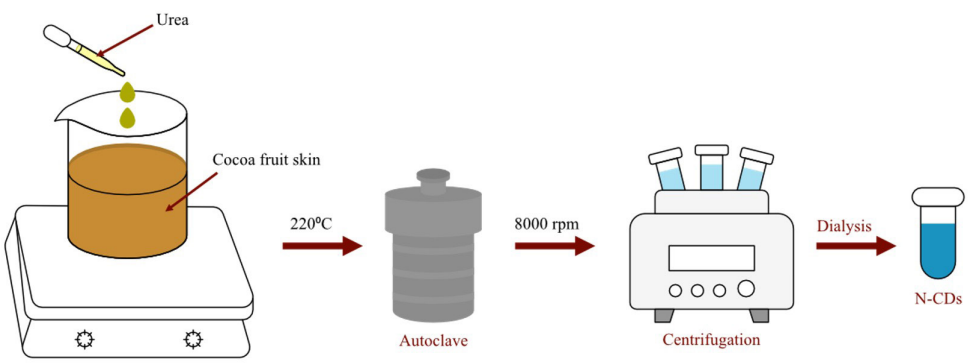

Figure 2. Schematic illustration synthesis N-CDs with the solvothermal method.

3.2 Morphology analysis

The TEM images and size distribution of CDs and N-CDs can be seen in Figure 3. The TEM images on the CDs (Figure 3a) show that the material is very well dispersed without forming aggregation. In the HR-TEM CDs (Figure 3b), it can see that the dots have formed. The spacing of the lattice fringe formed is around 0.23 nm, corresponding to graphite's diffraction (100)[23]. It shows that CDs are formed to resemble graphite in structure. The size distribution of CDs (Figure 3e) shows a size range of 2.52 nm. TEM images on N-CDs (Figure 3c) show that the material is dispersed well without forming aggregates. Looking at the HR-TEM N-CDs (Figure 3d), it can see that the dots have formed. The spacing of the lattice fringe formed is around 0.23 nm, corresponding to graphite's diffraction (100)[24]. It shows that the N-CDs are formed to resemble graphite structures. The size distribution of N-CDs (Figure 3f) shows a size range of 2.58 nm. The addition of elemental N to CDs did increase the particle size, although not significantly[25]. Bai et al.[26] also compared the sizes of CDs and N-CDs, and it was found that adding N to CDs increased the particle size. Das et al.[27] compared the addition of N elements to CDs, and it was found that the more N elements in CDS, the more the particle size would also increase, although not significantly. XRD results revealed a broad and prominent diffraction peak at $2\theta = 25.56°$[28], corresponding to the (002) crystal plane of graphite. This indicates the amorphous nature of the N-CDs, characterized by a non-crystalline structure of disordered carbon atoms. This amorphous structure is attributed to the incorporation of nitrogen and the solvothermal synthesis conditions, both of which disrupt the formation of graphite layers.

3.3 FTIR and EDS analysis

FTIR spectra can be seen in Figure 4 to confirm the surface function group for CDs and N-CDs. It is known that there is an adsorption band at 3324 cm-1, which shows O-H on both CDs and N-CDs. The adsorption band at 3324 cm^{-1} also shows asymmetric N-H stretching on the N-CDs[29]. The peaks of 2944 cm^{-1} and 2832 cm^{-1} show C-H stretching vibrations. The adsorption peak at 1654 cm^{-1} corresponds to C=O, and the adsorption peak at 1013 cm^{-1} corresponds to C-O. There is adsorption at 1409 cm^{-1} for the C-C bond. The adsorption peak difference between CDs and N-CDs is 1118 cm^{-1}, indicating C-N stretching[30]. FTIR spectra of N-CDS showed variations of the COOH, OH, and NH_2 functional groups. It can provide excellent stability in aqueous solutions[29].

EDS analysis (Figure 4) confirmed the composition of the sample elements. The results show that the carbon dots (CDs) primarily consist of carbon (C) at 58.51 atomic% and oxygen (O) at 16.29 atomic%, thus validating the successful synthesis of CDs[31]. Trace amounts of sodium (Na) and potassium (K) were also detected, likely contaminants from the glass slide used for analysis. The oxygen content in the synthesised CDs is attributed to the hydroxyl and carbonyl groups present in cocoa skin, the source material. Notably, the absence of nitrogen (N) peaks suggests a low nitrogen concentration in the EDS spectrum.

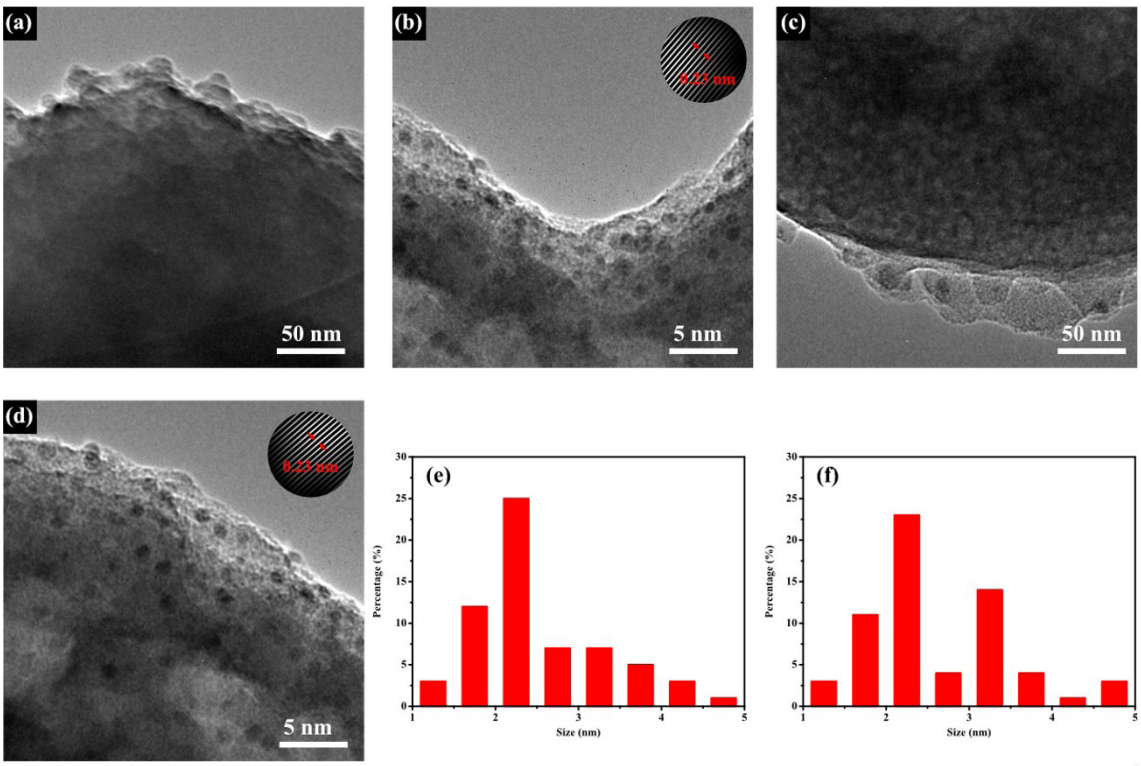

Figure 3. Morphological of (a) TEM images CDs, (b) HR TEM CDs, (c) TEM images N-CDs, (d) HR TEM N-CDs, (e) size distribution CDs, and (f) size distribution N-CDs.

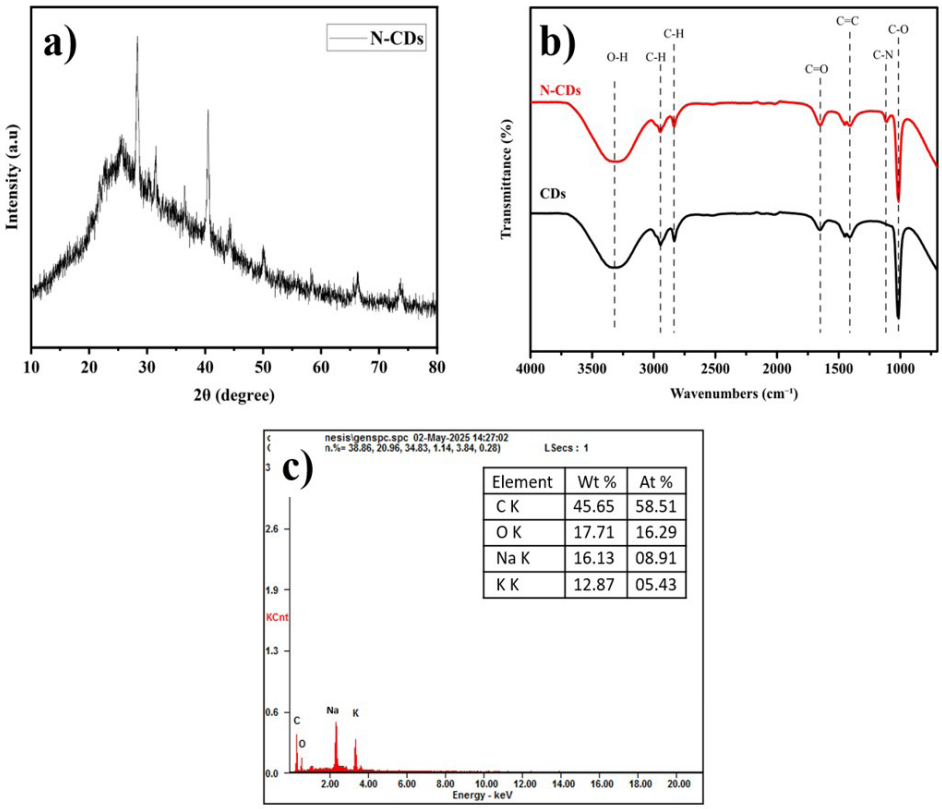

Figure 4. (a) XRD spectra of N-CDs, (b) FTIR spectra of CDS and N-CDs, and (c) EDS spectra of N-CDs.

3.4 UV-Vis analysis

UV-Vis absorption spectrum can be seen in Figure 5. In UV-Vis adsorption, and it can be seen the formation of curves on the long adsorption edge in the 300-600 nm region. CDs and N-CDs form peaks at 312 nm and 350 nm showing n-π* non-conjugated electron orbitals originating from oxygen bonding groups (C=O) or amino groups that occur in N-CDs[32]. The difference in the UV-Vis spectra of CDs and N-CDs is that the N-CDs show the formation of a peak at 294 nm, which shows the π-π* transition of sp^2, which is hybridized carbon core[33]. The exposed to around 350 nm in the UV-Vis absorption spectrum, the well-dispersed CDs and N-CDs showed blue emission, respectively. It shows that the emission depends on the size of the particles and the sp^2 carbon framework[34]. It was also shown that the more extensive conjugated system and the higher graphitization of the nitrogen-doped polyaromatic structure were important in lowering the energy bandgap. N–CDs have strong blue emissions that can be seen with the human eye. It is a good candidate for use in various fields, including bioimaging, biomedicine, and chemical sensing.

3.5 PL analysis

The PL spectra of CDs and N-CDs that are excited at 350 nm can be seen in Figure 6a. From the graph, it show that N–CDs had a more significant emission than CDs with the same absorption. Figure 6b shows that the highest PL QY of N–CDs in a water solution was about 18.25%. It was better than the highest fluorescence QY CDs, 8.00%. The QY on CDs is 8.18%. However, when added, urea increased the QY on N-CDs by 18.25% during synthesis. Simões et al.[35] also synthesized N-CDs, and it was found that the QY increased, originally QY CDs by 8%, QY NCDs increased by 12%. Likewise, Wang et al.[36] previously showed that QY CDs were 6.05%, but QY N-CDs were 18.79%. It was shown that urea did not produce emissions when it was made by hydrothermal synthesis on its own. It showed how important it is to use urea as a surface passivating agent and source of nitrogen to improve the PL features of N-CDs.

The selective light spectrum of CDs can be seen in Figure 6c. The excited by light with different excitation values (300-380 nm). The excitation frequency was less than 350 nm, and the emission peaks moved to the blue. Figure 6d shows how the selective light spectrum of N-CDs looks. The excited by light with different excitation values (300-380 nm), comprehensive emission features could be seen, in which the excitation rose to a maximum of 350 nm and then dropped quickly. The excitation frequency was less than 350 nm, and the emission peaks moved to the blue. This excitation dependence/independence emission range was probably caused by the surface state emission from the many reactive oxygen/nitrogen functional groups, which changes the energy bandgap of N–CDs[37]. Also, the selected luminescence excitation wavelength could have been caused by the difference in the size of the sp^2 hybridized carbon framework and the amount of nitrogen in the graphitic structure[38].

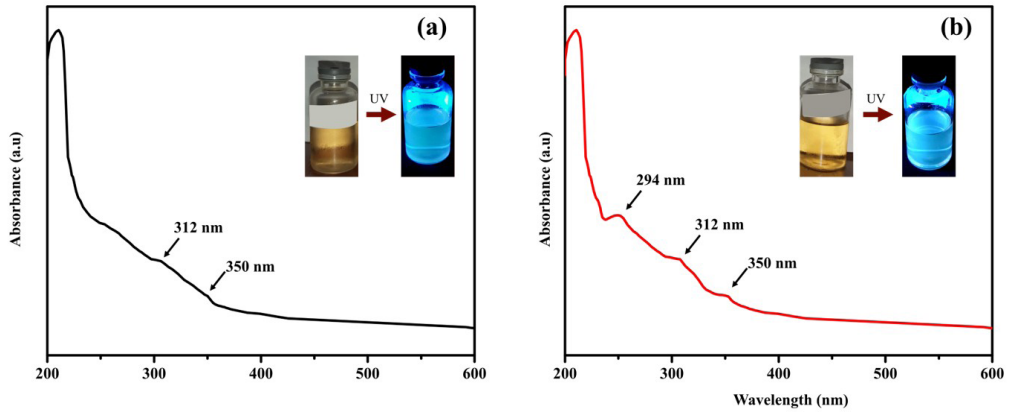

Figure 5. UV-Vis absorption spectrum of (a) CDs and (b) N-CDs.

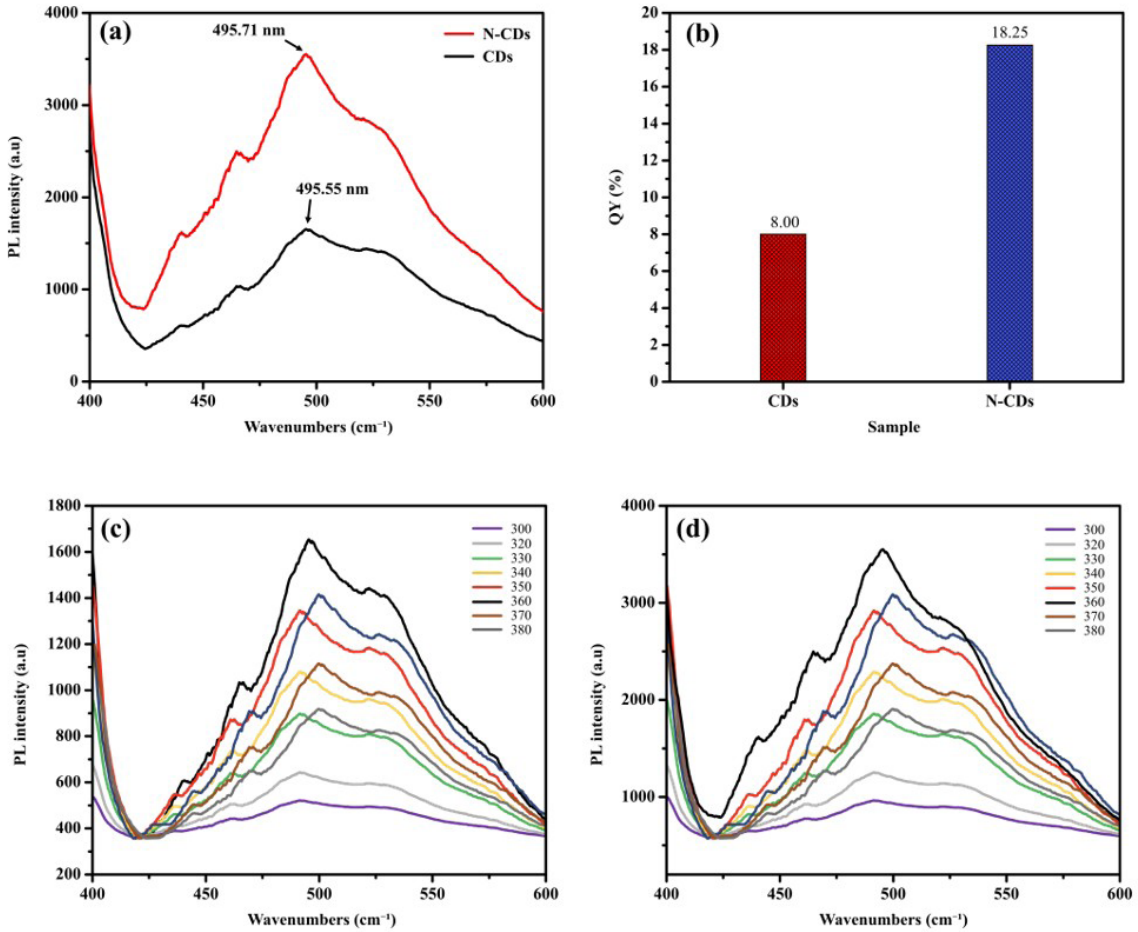

Figure 6. (a) Fluorescence PL spectra of CDs and N-CDs excited at 350 nm, (b) Quantum yield of CDs and N-CDs, (c) PL spectra of CDs under various excitation wavelengths (300-380 nm), and (d) PL spectra of N–CDs under various excitation wavelengths (300-380 nm).

3.6 Antibacterial study

The CDs and N-CDs carried out an antibacterial test. Streptomycin sulphate was used as a control for the antimicrobial study, and the size of the wells was 6 mm. We used the well-known and easy-to-use Agar-diffusion disk method for antibacterial strains in this method. Gram-positive and Gram-negative bacteria, both used in this study, are two types of these bacteria. Human bacteria like *Staphylococcus aureus* and *Escherichia coli* have been used to get CDs, and N-CDs can be seen in Figure 7. It has been

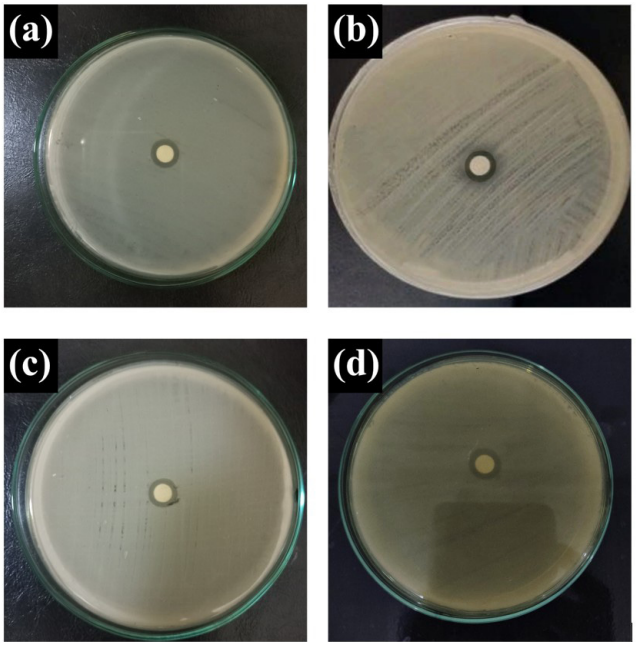

Figure 7. CDs involved against human pathogens of (a) *Staphylococcus aureus*, (b) *Escherichia coli*, and N-CDs involved against human pathogens of (c) *Staphylococcus aureus*, (d) *Escherichia coli* in concentrations in 100 µg.

Table 2. The zone of inhibition of CDs and N-CDs was involved in gram-positive and gram-negative human pathogens in concentrations of 100 µg.

Variant	Human pathogens	Standard antibiotic	Sample	The concentration of CDs and N-CDs (µg mL^{-1})
Gram +	*Staphylococcus aureus*	13.2 ± 0.80	CDs	7.3 ± 0.16
			N-CDs	10.5 ± 0.82
Gram -	*Escherichia coli*	13.2 ± 0.50	CDs	9.1 ± 0.13
			N-CDs	10.9 ± 0.97

seen that N-CDs work very quickly and kill many bacteria compared to CDs. In both CDs, the highest value for the zone of inhibition is 100 µg mL^{-1}. Table 2 shows the zone of inhibition for gram-negative and gram-positive bacterial species. Different band gaps between the N-CDs due to their ground and excited states reduce the formation of highly reactive oxygen species (ROS) and lessen their ability to kill bacteria in their respective applications[39]. N-CDs do have an advantage as an antibacterial when compared to CDs. Several studies have also concluded that N-CDs have good antibacterial properties. Rajapandi et al.[40] tested antibacterial N-CDs and CDs and showed that N-CDs had a better antibacterial ability. Wen et al.[41] researched N-CDs and added curcumin to increase the antibacterial ability compared to CDs.

4. Conclusion

N-Doped Carbon Dots From Cocoa Fruit Skin has been successfully synthesized. Phytochemical results in cocoa fruit skin contain alkaloids, flavonoids, terpenoids, saponins, tannins, and polyphenols. TEM images on N-CDs show the material is dispersed well without forming aggregation. The spacing of the lattice fringe formed is around 0.23 nm, corresponding to graphite's diffraction (100). FTIR spectra show adsorption peak difference between CDs and N-CDs is 1118 cm^{-1}, indicating C-N stretching. UV-Vis absorption spectrum shows the formation of a peak at 294 nm, which shows the π-π* transition of sp^2, which is hybridized carbon core. PL QY of N–CDs in a water solution was about 18.25%. The excitation dependence/independence emission range was probably caused by the surface state emission from the many reactive oxygen/nitrogen functional groups, which changes the energy bandgap of N–CDs. Also, the selected luminescence excitation wavelength could have been caused by the difference in the size of the sp^2 hybridized carbon framework and the amount of nitrogen in the graphitic structure. It has been seen that N-CDs work very quickly and kill many bacteria compared to CDs. In both CDs, the highest value for the zone of inhibition is 100 µg mL^{-1}.

5. Author's Contribution

- **Conceptualization** – Marpongahtun; Amru Daulay; Putri; Aniza Salviana Prayugo; Roon Goei, Salmiati.
- **Data curation** – Marpongahtun; Amru Daulay; Putri; Aniza Salviana Prayugo; Roon Goei, Salmiati.
- **Formal analysis** – Marpongahtun; Amru Daulay; Putri.

- **Funding acquisition** – Marpongahtun.
- **Investigation** – Marpongahtun; Amru Daulay; Putri; Aniza Salviana Prayugo; Roon Goei, Salmiati.
- **Methodology** – Marpongahtun; Amru Daulay; Putri.
- **Project administration** – Marpongahtun; Amru Daulay; Putri; Aniza Salviana Prayugo; Roon Goei, Salmiati.
- **Resources** – Marpongahtun; Amru Daulay; Putri; Roon Goei.
- **Software** – Marpongahtun; Amru Daulay; Putri.
- **Supervision** – Marpongahtun; Amru Daulay; Putri; Aniza Salviana Prayugo; Roon Goei, Salmiati.
- **Validation** – Marpongahtun; Amru Daulay; Putri; Aniza Salviana Prayugo; Roon Goei, Salmiati.
- **Visualization** – Marpongahtun; Amru Daulay; Putri; Aniza Salviana Prayugo; Roon Goei, Salmiati.
- **Writing – original draft** – Marpongahtun; Amru Daulay; Putri.
- **Writing – review & editing** – Marpongahtun; Amru Daulay; Putri; Aniza Salviana Prayugo; Roon Goei, Salmiati.

6. Acknowledgements

The authors acknowledge the support from Universitas Sumatera Utara and the School of Material Science and Engineering and Nanyang Technological University, in conducting material characterization.

7. References

1. Rachmawaty, Mu'nisa, A., Hasri, Pagarra, H., Hartati, & Maulana, Z. (2018). Active compounds extraction of cocoa pod husk (*Theobroma cacao* L.) and potential as fungicides. *Journal of Physics: Conference Series*, *1028*, 012013. http://doi.org/10.1088/1742-6596/1028/1/012013.
2. Mael, S. H. (2024). Cocoa pod husk meal as a feed ingredient for livestock. *Food and Energy Security*, *13*(5), e70003. http://doi.org/10.1002/fes3.70003.
3. Yuli, Y., & Eka, S., Rakiman, & Yazmendra, R. (2021). Biomass waste of cocoa skin for basic activated carbon as source of eco-friendly energy storage. *Journal of Physics: Conference Series*, *1788*, 012020. http://doi.org/10.1088/1742-6596/1788/1/012020.
4. Liu, J., Li, R., & Yang, B. (2020). Carbon dots: a new type of carbon-based nanomaterial with wide applications. *ACS Central Science*, *6*(12), 2179-2195. http://doi.org/10.1021/acscentsci.0c01306. PMid:33376780.
5. Zhao, F., Liu, Z., Sui, S., Huang, K., Yang, Y., Chen, Z., & Yin, H. (2023). Surficial amino groups coupling induced concentration-dependent fluorescence and fluorescence quantum yield of nitrogen-doped carbon quantum dots via efficient charge transfer. *Spectrochimica Acta. Part A: Molecular and Biomolecular Spectroscopy*, *294*, 122542. http://doi.org/10.1016/j.saa.2023.122542. PMid:36848858.
6. Desai, M. L., Jha, S., Basu, H., Singhal, R. K., Park, T.-J., & Kailasa, S. K. (2019). Acid oxidation of muskmelon fruit for the fabrication of carbon dots with specific emission colors for recognition of Hg^{2+} ions and cell imaging. *ACS Omega*, *4*(21), 19332-19340. http://doi.org/10.1021/acsomega.9b02730. PMid:31763557.
7. Chen, Z.-W., Hsieh, T.-H., & Liu, C.-P. (2022). Production of carbon dots by pulsed laser ablation: precursors and photo-oxidase properties. *Journal of the Chinese Chemical Society*, *69*(1), 193-199. http://doi.org/10.1002/jccs.202100271.
8. Pramudita, R., Marpongahtun, Gea, S., Daulay, A., Harahap, M., Tan, Y. Z., Goei, R., & Tok, A. I. Y. (2022). Synthesis of fluorescent citric acid carbon dots composites derived from empty fruit bunches of palm oil tree and its anti-bacterial property. *Case Studies in Chemical and Environmental Engineering*, *6*, 100277. http://doi.org/10.1016/j.cscee.2022.100277.
9. Marpongahtun, S., Siregar, I. P. H., Irham, W. H., & Saragih, S. W. (2023). Improving carbon dots optical properties of molasses using EDTA as a passivation agent with the microwave method. *Rasayan Journal of Chemistry*, *16*(2), 826-832. http://doi.org/10.31788/RJC.2023.1628237.
10. Wang, C.-I., Wu, W.-C., Periasamy, A. P., & Chang, H.-T. (2014). Electrochemical synthesis of photoluminescent carbon nanodots from glycine for highly sensitive detection of hemoglobin. *Green Chemistry*, *16*(5), 2509-2514. http://doi.org/10.1039/c3gc42325e.
11. Otten, M., Hildebrandt, M., Kühnemuth, R., & Karg, M. (2022). Pyrolysis and solvothermal synthesis for carbon dots: role of purification and molecular fluorophores. *Langmuir*, *38*(19), 6148-6157. http://doi.org/10.1021/acs.langmuir.2c00508. PMid:35502848.
12. Kurian, M., & Paul, A. (2021). Recent trends in the use of green sources for carbon dot synthesis: a short review. *Carbon Trends*, *3*, 100032. http://doi.org/10.1016/j.cartre.2021.100032.
13. Jing, H. H., Bardakci, F., Akgöl, S., Kusat, K., Adnan, M., Alam, M. J., Gupta, R., Sahreen, S., Chen, Y., Gopinath, S. C. B., & Sasidharan, S. (2023). Green carbon dots: Synthesis, characterization, properties and biomedical applications. *Journal of Functional Biomaterials*, *14*(1), 27. http://doi.org/10.3390/jfb14010027. PMid:36662074.
14. Wang, Y., Wu, R., Zhang, Y., Cheng, S., & Zhang, Y. (2023). High quantum yield nitrogen doped carbon dots for Ag^{+} sensing and bioimaging. *Journal of Molecular Structure*, *1283*, 135212. http://doi.org/10.1016/j.molstruc.2023.135212.
15. Tariq, M., Singh, A., Varshney, N., Samanta, S. K., & Sk, M. P. (2022). Biomass-derived carbon dots as an emergent antibacterial agent. *Materials Today. Communications*, *33*, 104347. http://doi.org/10.1016/j.mtcomm.2022.104347.
16. Sato, K., Katakami, R., Iso, Y., & Isobe, T. (2022). Surface-modified carbon dots with improved photoluminescence quantum yield for color conversion in white-light-emitting diodes. *ACS Applied Nano Materials*, *5*(6), 7664-7669. http://doi.org/10.1021/acsanm.2c01868.
17. Meng, J., Li, S., Ding, L., Zhou, C., Jiang, R., Zhang, Q., Cheng, Z., Gauthier, M., Hu, Y., & Wu, L. (2022). Preparation of nitrogen-doped carbon dots from coke powder as a fluorescent chemosensor for selective and sensitive detection of Cr (VI). *Journal of Wuhan University of Technology, Materials Science Edition*, *37*(6), 1096-1104. http://doi.org/10.1007/s11595-022-2639-3.
18. Saravanan, A., Maruthapandi, M., Das, P., Luong, J. H. T., & Gedanken, A. (2021). Green synthesis of multifunctional carbon dots with antibacterial activities. *Nanomaterials*, *11*(2), 369. http://doi.org/10.3390/nano11020369. PMid:33540607.
19. Prayugo, A. S., Marpongahtun, Gea, S., Daulay, A., Harahap, M., Siow, J., Goei, R., & Tok, A. I. Y. (2023). Highly fluorescent nitrogen-doped carbon dots derived from jengkol peels (*Archidendron pauciflorum*) by solvothermal synthesis for sensitive Hg^{2+} ions detection. *Biosensors and Bioelectronics: X*, *14*, 100363. http://doi.org/10.1016/j.biosx.2023.100363.
20. Adu, J. K., Amengor, C. D. K., Kabiri, N., Orman, E., Patamia, S. A. G., & Okrah, B. K. (2019). Validation of a simple and robust Liebermann-Burchard colorimetric method for the assay of cholesterol in selected milk products in Ghana. *International Journal of Food Sciences*, *2019*(1), 9045938. http://doi.org/10.1155/2019/9045938. PMid:31737650.

21. Feng, S.-H., & Li, G.-H. (2017). *Hydrothermal and solvothermal syntheses*. In R. Xu, & Y. Xu (Eds.), *Modern inorganic synthetic chemistry* (pp. 73-104). Amsterdam: Elsevier. http://doi.org/10.1016/B978-0-444-63591-4.00004-5.
22. Monday, Y. N., Abdullah, J., Yusof, N. A., Rashid, S. A., & Shueb, R. H. (2021). Facile hydrothermal and solvothermal synthesis and characterization of nitrogen-doped carbon dots from palm kernel shell precursor. *Applied Sciences*, *11*(4), 1630. http://doi.org/10.3390/app11041630.
23. Guo, J., Qin, L., & Wang, D. (2023). Carbon dots preserve strong blue emission in both aqueous and solid states and their application in intracellular temperature sensing and white light-emitting diodes. *Journal of Luminescence*, *257*, 119690. http://doi.org/10.1016/j.jlumin.2023.119690.
24. Li, C., Liang, H., Bai, S., Zhu, J., Chen, Z., Yang, G., & Zhu, Y. (2023). Efficient color-tunable room temperature phosphorescence through carbon dot confinement in urea crystals. *Journal of Luminescence*, *254*, 119497. http://doi.org/10.1016/j.jlumin.2022.119497.
25. Nguyen, K. G., Baragau, I.-A., Gromicova, R., Nicolaev, A., Thomson, S. A. J., Rennie, A., Power, N. P., Sajjad, M. T., & Kellici, S. (2022). Investigating the effect of N-doping on carbon quantum dots structure, optical properties and metal ion screening. *Scientific Reports*, *12*(1), 13806. http://doi.org/10.1038/s41598-022-16893-x. PMid:35970901.
26. Bai, J., Xiao, N., Wang, Y., Li, H., Liu, C., Xiao, J., Wei, Y., Guo, Z., & Qiu, J. (2021). Coal tar pitch derived nitrogen-doped carbon dots with adjustable particle size for photocatalytic hydrogen generation. *Carbon*, *174*, 750-756. http://doi.org/10.1016/j.carbon.2020.10.088.
27. Das, D., & Dutta, R. K. (2021). N-doped carbon dots synthesized from ethylene glycol and β-alanine for detection of Cr(VI) and 4-nitrophenol via photoluminescence quenching. *ACS Applied Nano Materials*, *4*(4), 3444-3454. http://doi.org/10.1021/acsanm.0c03329.
28. Cai, D., Zhong, X., Xu, L., Xiong, Y., Deng, W., Zou, G., Hou, H., & Ji, X. (2025). Biomass-derived carbon dots: synthesis, modification and application in batteries. *Chemical Science*, *16*(12), 4937-4970. http://doi.org/10.1039/D4SC08659G. PMid:40046072.
29. Liu, X., Liu, J., Zheng, B., Yan, L., Dai, J., Zhuang, Z., Du, J., Guo, Y., & Xiao, D. (2017). N-doped carbon dots: green and efficient synthesis on a large scale and their application in fluorescent pH sensing. *New Journal of Chemistry*, *41*(19), 10607-10612. http://doi.org/10.1039/C7NJ01889D.
30. Jenab, A., Roghanian, R., Ghorbani, N., Ghaedi, K., & Emtiazi, G. (2020). The efficacy of electrospun PAN/kefiran nanofiber and kefir in mammalian cell culture: promotion of PC12 cell growth, anti-MCF7 breast cancer cells activities, and cytokine production of PBMC. *International Journal of Nanomedicine*, *15*, 717-728. http://doi.org/10.2147/IJN.S232264. PMid:32099360.
31. Mansuriya, B. D., & Altintas, Z. (2021). Carbon dots: classification, properties, synthesis, characterization, and applications in health care: an updated review (2018-2021). *Nanomaterials*, *11*(10), 2525. http://doi.org/10.3390/nano11102525. PMid:34684966.
32. Issa, M. A., Abidin, Z. Z., Sobri, S., Rashid, S., Mahdi, M. A., Ibrahim, N. A., & Pudza, M. Y. (2019). Facile synthesis of nitrogen-doped carbon dots from lignocellulosic waste. *Nanomaterials*, *9*(10), 1500. http://doi.org/10.3390/nano9101500. PMid:31652527.
33. Li, Y., Liu, C., Chen, M., Zheng, Y., Tian, H., Shi, R., He, X., & Lin, X. (2022). Preparing colour-tunable tannic acid-based carbon dots by changing the pH value of the reaction system. *Nanomaterials*, *12*(17), 3062. http://doi.org/10.3390/nano12173062. PMid:36080100.
34. Li, X. (2021). sp^2 carbon-conjugated covalent organic frameworks: Synthesis, properties, and applications. *Materials Chemistry Frontiers*, *5*(7), 2931-2949. http://doi.org/10.1039/D1QM00015B.
35. Simões, E. F. C., Leitão, J. M. M., & Silva, J. C. G. E. (2016). Carbon dots prepared from citric acid and urea as fluorescent probes for hypochlorite and peroxynitrite. *Mikrochimica Acta*, *183*(5), 1769-1777. http://doi.org/10.1007/s00604-016-1807-6.
36. Wang, K., Geng, C., Wang, F., Zhao, Y., & Ru, Z. (2021). Urea-doped carbon dots as fluorescent switches for the selective detection of iodide ions and their mechanistic study. *RSC Advances*, *11*(44), 27645-27652. http://doi.org/10.1039/D1RA04558J. PMid:35480658.
37. Olla, C., Cappai, A., Porcu, S., Stagi, L., Fantauzzi, M., Casula, M. F., Mocci, F., Corpino, R., Chiriu, D., Ricci, P. C., & Carbonaro, C. M. (2023). Exploring the impact of nitrogen doping on the optical properties of carbon dots synthesized from citric acid. *Nanomaterials*, *13*(8), 1344. http://doi.org/10.3390/nano13081344. PMid:37110929.
38. Ray, P., Moitra, P., & Pan, D. (2022). Emerging theranostic applications of carbon dots and its variants. *View*, *3*(2), 20200089. http://doi.org/10.1002/VIW.20200089.
39. Quan, L., Jiang, W., Li, H., Li, H., Wang, Q., & Chen, L. (2022). Intelligent intra-row robotic weeding system combining deep learning technology with a targeted weeding mode. *Biosystems Engineering*, *216*, 13-31. http://doi.org/10.1016/j.biosystemseng.2022.01.019.
40. Rajapandi, S., Pandeeswaran, M., & Kousalya, G. N. (2022). Novel green synthesis of N-doped carbon dots from fruits of *Opuntia ficus-indica* as an effective catalyst for the photocatalytic degradation of methyl orange dye and antibacterial studies. *Inorganic Chemistry Communications*, *146*, 110041. http://doi.org/10.1016/j.inoche.2022.110041.
41. Wen, F., Li, P., Meng, H., Yan, H., Huang, X., Cui, H., & Su, W. (2022). Nitrogen-doped carbon dots/curcumin nanocomposite for combined photodynamic/photothermal dual-mode antibacterial therapy. *Photodiagnosis and Photodynamic Therapy*, *39*, 103033. http://doi.org/10.1016/j.pdpdt.2022.103033. PMid:35905831.

Received: Feb. 19, 2025
Revised: June 05, 2025
Accepted: June 11, 2025

Associate Editor: Sebastião V. Canevarolo